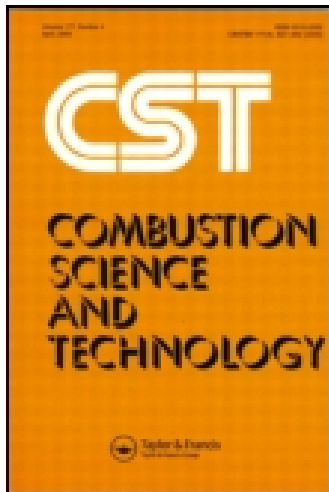


This article was downloaded by: [National Forest Service Library]

On: 13 February 2015, At: 11:20

Publisher: Taylor & Francis

Informa Ltd Registered in England and Wales Registered Number: 1072954 Registered office: Mortimer House, 37-41 Mortimer Street, London W1T 3JH, UK



## Combustion Science and Technology

Publication details, including instructions for authors and subscription information:

<http://www.tandfonline.com/loi/gcst20>

### An Investigation of the Influence of Heating Modes on Ignition and Pyrolysis of Woody Wildland Fuel

B. L. Yashwanth<sup>a</sup>, B. Shotorban<sup>a</sup>, S. Mahalingam<sup>a</sup> & D. R. Weise<sup>b</sup>

<sup>a</sup> Department of Mechanical and Aerospace Engineering, The University of Alabama in Huntsville, Huntsville, Alabama, USA

<sup>b</sup> Pacific Southwest Research Station, USDA Forest Service, Riverside, California, USA

Accepted author version posted online: 22 Dec 2014.



CrossMark

[Click for updates](#)

To cite this article: B. L. Yashwanth, B. Shotorban, S. Mahalingam & D. R. Weise (2015) An Investigation of the Influence of Heating Modes on Ignition and Pyrolysis of Woody Wildland Fuel, *Combustion Science and Technology*, 187:5, 780-796, DOI: [10.1080/00102202.2014.973948](https://doi.org/10.1080/00102202.2014.973948)

To link to this article: <http://dx.doi.org/10.1080/00102202.2014.973948>

PLEASE SCROLL DOWN FOR ARTICLE

Taylor & Francis makes every effort to ensure the accuracy of all the information (the "Content") contained in the publications on our platform. However, Taylor & Francis, our agents, and our licensors make no representations or warranties whatsoever as to the accuracy, completeness, or suitability for any purpose of the Content. Any opinions and views expressed in this publication are the opinions and views of the authors, and are not the views of or endorsed by Taylor & Francis. The accuracy of the Content should not be relied upon and should be independently verified with primary sources of information. Taylor and Francis shall not be liable for any losses, actions, claims, proceedings, demands, costs, expenses, damages, and other liabilities whatsoever or howsoever caused arising directly or indirectly in connection with, in relation to or arising out of the use of the Content.

This article may be used for research, teaching, and private study purposes. Any substantial or systematic reproduction, redistribution, reselling, loan, sub-licensing, systematic supply, or distribution in any form to anyone is expressly forbidden. Terms &

Conditions of access and use can be found at <http://www.tandfonline.com/page/terms-and-conditions>

## AN INVESTIGATION OF THE INFLUENCE OF HEATING MODES ON IGNITION AND PYROLYSIS OF WOODY WILDLAND FUEL

B. L. Yashwanth,<sup>1</sup> B. Shotorban,<sup>1</sup> S. Mahalingam,<sup>1</sup>  
and D. R. Weise<sup>2</sup> 

<sup>1</sup>Department of Mechanical and Aerospace Engineering, The University of Alabama in Huntsville, Huntsville, Alabama, USA

<sup>2</sup>Pacific Southwest Research Station, USDA Forest Service, Riverside, California, USA

*The ignition of woody wildland fuel modeled as a one-dimensional slab subject to various modes of heating was investigated using a general pyrolysis code, Gpyro. The heating mode was varied by applying different convective and/or radiative, time-dependent heat flux boundary conditions on one end of the slab while keeping the other end insulated. Dry wood properties were used for the slab. Initially, wood was treated as chemically inactive and following this it is presumed to decompose via a single-stage kinetic model involving two solid phase species coupled with one gas phase species. This single-step model approximation for wood degradation was validated with experimental results. Critical time was defined as the time when the temperature of the heated side reached a critical value at which the ignition was assumed to take place. The chemically inactive assumption led to a significant underprediction of the critical time for a broad range of convective heat source temperatures at a fixed Biot number. When thermal decomposition was included, the critical time was quite sensitive to radiative and convective source temperatures and the Biot number during combined mode of heating. Time evolution of the mass loss and charring rates was weakly influenced by convective heating during the combined mode of heating. The variation of Biot number had little influence on this evolution when a combined mode of heating was applied.*

**Keywords:** Charring rate; Ignition time; Mass loss rate; Wildland fire; Wood combustion

### 1. INTRODUCTION

Examining the ignition behavior of woody fuel under different heating conditions would help in determining the effective mode of heating that could result in ignition during a wildland fire, and this can later be extended to investigate its effects on fire intensity and spread rate. Key ignition criteria identified for woody materials are surface ignition temperature, critical mass flux of volatiles, and critical heat flux (Babrauskas, 2001). The temperature at which wood decomposition is initiated is referred to as the critical temperature (Lawson and Simms, 1952; Simms and Law, 1960) and the time taken for it to

Received 25 December 2013; revised 30 August 2014; accepted 3 October 2014.

Address correspondence to B. Shotorban, Department of Mechanical and Aerospace Engineering, The University of Alabama in Huntsville, Huntsville, AL 35899, USA. E-mail: babak.shotorban@uah.edu

reach this temperature is referred to as the critical time. A number of previous publications have focused on critical time (Atreya et al., 1986; Babrauskas, 2001; Bilbao et al., 2002; Brescianini et al., 2003; Delichatsios et al., 2003; Moghtaderi et al., 1997; Thomson et al., 1988), heating mode (Babu and Chaurasia, 2003; Frankman et al., 2010; Lizhong et al., 2007; Tan et al., 2009), and mass loss rate (Delichatsios, 2005; Lautenberger and Fernandez-Pello, 2009; McAlister et al., 2012; Shen et al., 2006). Many of these studies were on pyrolysis and/or combustion models with an ignition criterion that utilized a critical surface temperature as the ignition temperature (Atreya et al., 1986; Bilbao et al., 2002; Frankman et al., 2010; Lautenberger and Fernandez-Pello, 2005; Thomson et al., 1988). Experiments of Atreya et al. (1986) and Thomson et al. (1988) showed that the critical time is approximately the same time at which the surface of the particle begins to undergo pyrolysis. According to Babrauskas (2001), the critical ignition temperature for wood varied from 210°C to 497°C mostly for piloted ignition, and from 220°C to 510°C for autoignition. Such a wide variation might be due to differences in the definition of ignition temperature; design of the test apparatus; and operating conditions, such as moisture content, orientation of fuel, and the species of wood (Frankman et al., 2010).

The relative importance of external heating modes in wildland fire has been long debated (Finney et al., 2013; Zhou et al., 2005). Anderson (1969) reported that radiation heat transfer accounted for no more than 40% of the total heat flux needed to maintain rate of spread in certain fuels. Pagni and Peterson (1973) formulated a model that included radiation, convection, and conduction heat transfer modes and compared the model output with laboratory results in pine needle fuel beds (Rothermel and Anderson 1966). In this model formulation under no-wind ambient conditions, radiation was dominant; but in wind-aided flame spread, convection was dominant. Due to the complexity of processes that occur concurrently during a fire, the role of these two different modes of heating and the balance between them remain largely misunderstood in the area of wildland fires (Frankman et al., 2010). Weber (1991) identified radiation heat transfer as the dominant heat transfer mode in wildland fires through a simple analytical model, and expressed the need for a short-range heat transfer mechanism for fires in still air. Dupuy (2000) used experiments to verify multiple radiation driven models to determine if radiation alone can describe experimental results when it is considered as the dominant heat transfer mechanism in flame spread. They concluded that a radiation-dominant model could not account for experimental observations. Butler et al. (2004a) reported direct measurements of energy transfer in full-scale crown fires. The data suggested that radiative heating could account for the bulk of the particle heating ahead of the flaming front; however, it was indicated that immediately prior to ignition, convective heating was significant and possibly required, for ignition. Anderson et al. (2010) reported an extensive set of wind tunnel experiments using porous beds of fine fuels wherein they focused on convective heating in advance of a spreading line fire. Their work showed that the gas temperature adjacent to a solid fuel particle remained below the solid fuel temperature until the flame was within a few centimeters of the fuel particle. In a recent work by Frankman et al. (2010) on heating modes, a parametric study was conducted using radiation as a heating source and convection as a cooling source. The limitation of this research is that it did not include convection as a heating mode, and furthermore, fine fuel was used for their study. Lawson and Simms (1952) studied the time taken for ignition of wood when subjected to different intensities of irradiation to aid in identifying key parameters for comparison with experimental results; however, the effect of convection as a source of heat was not explored.

In a wildland fire, heating of unburned vegetation ahead of a fire front involves both convection from the flame contact and radiation; however, both modes of heating are transient and vary in magnitude as wind gusts (hot gases) and intensity of burning of the vegetation might increase, increasing the overall magnitude of convection and radiation respectively. In such a case, a clear balance between the different time varying sources of heating and their effective role in ignition and fire spread is not well understood. Most of the research reported to date considered the influence of constant external heat flux on ignition time, mass loss rate (MLR), and charring rate, without explicitly focusing on differences due to modes of heating and their time varying nature (Benkoussas et al., 2007; Bilbao et al., 2002; Haseli et al., 2012). The main goal of the present work is to investigate the role of different magnitudes of radiation and convection modes as sources of heating of a slab of woody fuel by observing their influence on critical time, MLR, and charring rate. Furthermore, the balance and effective role played by each mode is analyzed.

In the present work, first, a case wherein wood is considered an inert thermally thick substance is studied. This is done in order to gain insight into the rate of change in surface temperature when the slab is subjected to a time-dependent radiative and convective heat source. Surface temperature response is one of the important criteria used for ignition and if this shows any variation in its response to heating mode and heating rate, it could imply that the thermal degradation and associated chemical activity preceding ignition may be directly influenced by this variation. In the second stage, the woody fuel slab is treated as a thermally-thick, chemically-active medium, and its detailed response to heating by different modes via examination of MLR, critical time, and charring rate is presented. The other side of the slab is insulated to serve as a symmetry boundary condition (Babu and Chaurasia, 2003).

## 2. PHYSICAL CONFIGURATION

In a spreading wildland fire, unburned vegetation that lies ahead of burning and burned vegetation is exposed to varying magnitudes of convective and radiative heating. The physical model considered in this article is designed to focus on this situation. Although idealized, the choice of this configuration involving a one-dimensional (1D) slab of woody material with fixed thickness is motivated in part by the simplicity it affords and its similarity to experimental configurations studied by McAllister et al. (2011, 2012). This configuration enables a computational investigation of critical time, MLR, and spread rate under the influence of different modes of heating.

A schematic of the physical domain along with the boundary conditions is shown in Figure 1. The woody fuel slab is considered dry and thermally thick with a thickness  $L$ . Related work has shown that the presence of water vapor can significantly alter ignition flame characteristics (Ferguson et al., 2013); however, this additional complicating factor is not included in the present setup. It is exposed to radiative and convective heating on one side ( $x = 0$ ) and insulated on the other side of the domain ( $x = L$ ). Here,  $T_\infty$  is the reference ambient air temperature for convective heating of the fuel slab, and likewise,  $T_h$  is the source or heater temperature responsible for radiative heating, and  $T_s$  is the time-varying surface temperature at  $x = 0$ . The symbol  $T_{\text{source}}$  denotes the relevant heating mode source temperature,  $T_\infty$  or  $T_h$ . In order to model the wind effects, a convective heat transfer coefficient  $h$  is considered. The domain is initially at a uniform temperature  $T_0 = 27^\circ\text{C}$ . Since we use critical temperature as the ignition criteria, the time at which surface temperature reaches this value  $T_{cr} = 370^\circ\text{C}$  (Babrauskas, 2001; Lautenberger and Fernandez-Pello, 2005), is

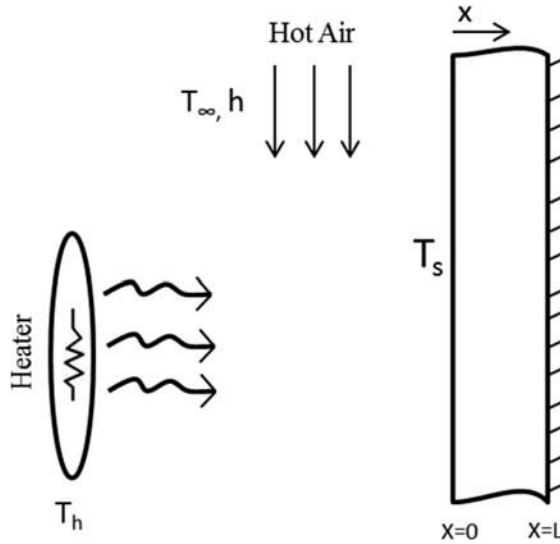


**Figure 1** Schematic diagram of the physical configuration. A 1D slab of woody fuel of width  $L$  is subject to heating by either convection (hot air), radiation (heater), or mixed mode heat transfer.

referred to here as critical time and is denoted by  $t_{cr}$ . It is noted that in this work, we are not dealing with flaming ignition for which the use of critical fuel mass flux is arguably a better criterion (McAllister et al., 2011; Rasbash et al., 1986). Our focus is to investigate ignition, regarded as the initiation of pyrolysis, which occurs prior to flaming combustion. Here, we would like to add that the previous works that used the critical mass flux, as an ignition criterion for flaming ignition, and suggested values for this flux are limited to cases where ignition is due to a pilot source (McAllister et al., 2011; Rasbash et al., 1986). The need for a pilot source to cause flaming combustion in the context of wildland fires is still an active area of research since wildland fires could also be a result of autoignition of fuel vapors.

### 3. MATHEMATICAL AND COMPUTATIONAL MODELS

#### 3.1. Chemically Inactive Media

Initially the woody fuel slab is assumed to be chemically inactive and analysis focuses on the initial preheating stage. It was assumed that the thermophysical properties of wood are constant and no chemical decomposition takes place before the surface at  $x = 0$  attains the critical temperature.

The governing equation is:

$$\rho c_p \frac{\partial T}{\partial t} = k \frac{\partial^2 T}{\partial x^2} \quad (1)$$

where  $T$  is temperature,  $t$  is time, and  $x$  is the 1D spatial coordinate. In Eq. (1),  $\rho$ ,  $c_p$ , and  $k$  are the density, heat capacity, and thermal conductivity. The boundary conditions (BC) are:

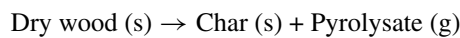
$$-k \frac{\partial T}{\partial x} \Big|_{x=0} = h(T_\infty - T_s) + \sigma \epsilon (T_h^4 - T_s^4) \quad (2)$$

$$-k \frac{\partial T}{\partial x} \Big|_{x=L} = 0 \quad (3)$$

and the initial condition is  $T(x, 0) = T_0$ . Here  $\sigma$  is the Stefan–Boltzmann constant,  $h$  is the heat transfer coefficient, and  $\epsilon$  is the emissivity. Convective heating mode is investigated by eliminating the radiation contribution on the right-hand side of Eq. (2). Likewise, radiation heating mode is investigated by eliminating the convective contribution in Eq. (2). Finally, combined or mixed mode heating is studied by including both terms. Dimensionless temperature, position, and time are defined as  $\theta \equiv T/T_0$ ,  $\xi \equiv x/L$ , and  $\tau \equiv \alpha t/L^2$ , respectively. Also,  $Bi = hL/k$  is the Biot number, and  $R = (\sigma \epsilon T_0^3 L)/k$  is a dimensionless number that characterizes external radiation (Tan et al., 2009). Thus,  $\theta_\infty$  and  $\theta_h$  denote the dimensionless source temperatures associated with the mode of heating, convective and radiative respectively, and the dimensionless time taken for the surface temperature  $\theta_s$  to reach critical temperature  $\theta_{s-cr}$  is  $\tau_{cr}$ . Lastly,  $\theta_{source}$  denotes the dimensionless heating mode source temperature  $\theta_\infty$  or  $\theta_h$ .

### 3.2. Chemically Active Media

The model outlined in Section 3.1 is extended so that the 1D fuel slab of woody material shown schematically in Figure 1 is presumed to be both thermally thick and chemically active. Wood is modeled as consisting of two solid phase species (wood and char) coupled to one gas phase species (pyrolysate). The ambient gas phase external to the decomposing woody fuel slab contributes only to convective heating. Thus, any reference to the gas phase, as far as the chemical reactions are concerned, pertains to the gases inside the pores or voids that form within decomposing wood. A single-stage reaction kinetic scheme considered by Lautenberger and Fernandez-Pello (2009) is used to model fuel decomposition in an anaerobic environment:



The model used by Lautenberger and Fernandez-Pello (2009) is primarily based on wood and can be applied in the context of wildland fires since it has been formulated using white pine wood, a common wildland fuel. Also, the value  $40 \text{ kW/m}^2$ , used by them for heat flux as one of the parameters, is typical of wildland fires. The values of the rest of the parameters, i.e., the kinetic parameters, are obtained through application of genetic algorithm optimization on the experimental data of Ohlemiller et al. (1987). The reaction given above is a reduced version of the two-step model employed by Lautenberger and Fernandez-Pello (2009). Their first-step reaction is for conversion of moist wood to dry wood while their second-step reaction is for conversion of dry wood to char. In the current work, we have used only their second-step reaction as we only consider dry wood. This reaction is endothermic and the thermophysical properties of wood and char are shown in Table 1. The values used for activation energy, pre-exponential factor, and heat of reaction are  $135 \text{ (kJ/mol)}$ ,  $3.29 \times 10^9 \text{ (s}^{-1}\text{)}$ , and  $5.33 \times 10^5 \text{ (J/kg)}$ , respectively (Lautenberger and Fernandez-Pello, 2009).

**Table 1** Thermophysical properties of the solid species at 25°C

Properties	Wood	Char
Density ( $\rho$ )	400 kg/m <sup>3</sup>	73 kg/m <sup>3</sup>
Thermal conductivity ( $k$ )	0.2 W/mK	0.065 W/mK
Specific heat ( $c_p$ )	1200 J/kgK	1216 J/kgK
Thermal diffusivity ( $\alpha$ )	$4.1 \times 10^{-7}$ m <sup>2</sup> s <sup>-1</sup>	$7.32 \times 10^{-7}$ m <sup>2</sup> s <sup>-1</sup>

This model, although simple, can be used to address the initial preheating stage during thermal breakdown of wood. To support this claim, a comparison was made between our simulation results obtained using this one-step reaction, experimental results of Ohlemiller et al. (1987), and numerical results of Lautenberger and Fernandez-Pello (2009). The computational set-up (not shown) used for this case is similar to Ohlemiller et al. (1987) and consists of a 1D slab of white pine irradiated with 40 kW/m<sup>2</sup> on one side and convectively cooled on the other. The heat transfer coefficient and the dimension of the slab used are 10 W/m<sup>2</sup>K and 3.8 cm, respectively (Lautenberger and Fernandez-Pello, 2009). As seen in Figure 2, temperatures obtained in the current study match reasonably well with the temperatures obtained by Ohlemiller et al. (1987) and Lautenberger and Fernandez-Pello (2009). This match confirms that the effect of drying phase reaction on temperature response is small, and hence, can be neglected.

The mathematical model with main assumptions, governing equations, and boundary conditions for the chemically-active case is described in detail elsewhere (Lautenberger and Fernandez-Pello, 2009). Only the essential features adapted for the present investigation are highlighted here. The governing equations involving the two solid phase and one gas phase species consist of conservation of mass of species expressed in terms of their mass fractions (two in the solid phase and one in the gas phase), an overall mass conservation equation in terms of mass averaged density for the solid and overall gas density in the gas phase, and a single conservation of energy. The solid phase and gas phase are considered to be in thermal equilibrium, and thus a single conservation of energy equation for the solid phase

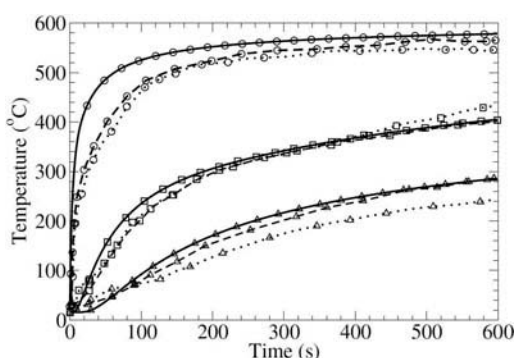


**Figure 2** Time history of temperatures of points at depths 0 mm (circle symbol), 5 mm (square symbol), and 10 mm (triangular symbol) from the surface of white pine irradiated at 40 kW/m<sup>2</sup> in nitrogen atmospheres in the configuration studied experimentally (dotted line) by Ohlemiller et al. (1987), computationally with a two-step reaction (dashed line) by Lautenberger and Fernandez-Pello (2009), and computationally with a single-step reaction in the present study (solid line).

suffices. The gas phase mass conservation equation is formulated using Darcy's law for the overall mass flux. The initial and boundary conditions for the solid-phase energy equation, expressed in terms of temperature, are identical to that discussed in Section 3.1. The solid phase species equations do not require any supporting boundary conditions. For the gas phase species, at  $x = L$ , zero flux or impermeable boundary conditions are imposed and at  $x = 0$ , a convective boundary condition is imposed.

### 3.3. Numerical Approach

In this study, Gpyro (2007), an open-source program, is utilized to solve the governing unsteady equations. Gpyro is capable of modeling thermochemical processes that occur in heated solids (Lautenberger and Fernandez-Pello, 2009). It can handle zero dimensional (lumped), 1D to 3D configurations with thermal and thermo-oxidative decomposition of solid-phase species. Gpyro utilizes a finite volume method for the spatial discretization of the governing equations. Time advancement is implicit and a tri-diagonal matrix algorithm (TDMA) scheme is used to solve the resulting system of algebraic equations in the case of a 1D problem as described here. First, Gpyro was utilized to solve the 1D chemically inert preheating problem outlined in Section 3.1. Second, it was used to solve the same configuration while taking into account the thermal decomposition of the chemically active media as presented in Section 3.2.

## 4. RESULTS AND DISCUSSION

The chemically inactive problem formulated in Section 3.1 has an infinite series solution in the case of convective mode heating (Bergman et al., 2011). This case was used to validate the computational method adopted here. The computed solution for a number of input parameters considered, not shown here, matched the analytical solution satisfactorily.

Figures 3a and 3b display the dependence of critical time as a function of the source temperature associated with the selected mode of heating and the total delivered energy to the slab over the course of the critical time for these situations. These simulations were carried out considering the material to be chemically inactive. In all cases, for a chosen  $\theta_{\text{source}}$ , the initial surface heat flux for the two heating modes are matched. The total energy delivered to the slab to raise the surface temperature to the critical temperature obtained as  $\int_0^{\tau_{\text{cr}}} \partial\theta/\partial\xi|_{\xi=0} d\tau$  is computed via a simple quadrature. From Figure 3a, it is evident that the critical time decreases with increasing source temperature for both modes of heating, consistent with expectation. This decrease is more than an order of magnitude for the range  $\theta_{\text{source}} = 2.3$  to 3.0 (corresponding to  $T_{\text{source}}$  of 690 K to 900 K). For a fixed value of the source temperature, the critical time for radiation mode heating is substantially smaller than that for convection, especially for smaller source temperatures. The variation of the critical time against the total delivered energy is displayed in Figure 3b. From Figures 3a and 3b, it is observed that higher source temperatures require less total energy delivered to the slab over the critical time period. Higher heating rates are attained at higher source temperatures; therefore, the material heats faster resulting in lower critical times. The inference here is that the heating process in the case of radiative BC is faster than in the case of convective BC. Also, the total amount of energy delivered until the temperature reaches the critical temperature in the case of radiative BC is less than in convective BC.

The dependence of the critical time as a function of the source temperature  $\theta_{\text{source}} = \theta_{\infty}$  under convective mode heating is shown in Figure 4 for both active and inert media.

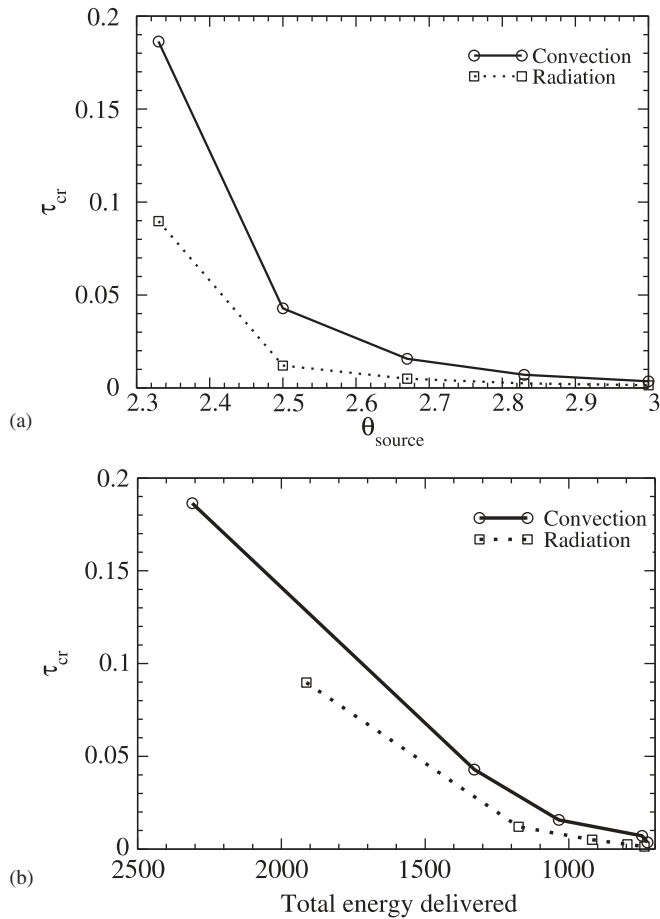


**Figure 3** Critical time against (a) heating source temperature ( $\theta_{source}$  represents  $\theta_h$  and  $\theta_\infty$  in radiation and convection heating, respectively) and (b) total energy delivered in chemically inert media.

Although the trends of the curves for both media are similar, the difference between them is significant. The reason could be attributed to the endothermic reaction used here for thermal breakdown. The chemically inactive approximation for the pure convection cases considered here is different from the chemically active results. Results discussed in the remainder of this section focus on a detailed parametric study of a chemically active media when it is subjected to different modes of heating. We examine convective and mixed mode heating process at constant  $\theta_h$  and Bi, and subsequently study radiation and mixed mode heating process at constant  $\theta_\infty$ . This approach helps in comparing different cases systematically, thereby providing a complete understanding of the entire problem.

In the case of chemically active media, the dependence of critical time on  $\theta_\infty$  is displayed in Figure 5 for various Bi numbers. In Figure 5a, the heating mode is only convection whereas in Figure 5b, it is mixed mode heating. The radiative heat source temperature is  $\theta_h = 3$  in all cases studied in Figure 5b. As seen in Figure 5a, the critical time reduces as the convective fluid temperature increases. The effect of the heat transfer coefficient has been also investigated here by considering various Bi numbers. Higher Bi numbers used here are

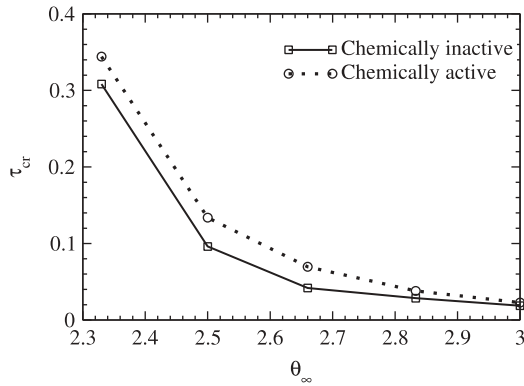


**Figure 4** The dependence of critical time on source temperature for convective mode of heating,  $Bi = 7.6$ .

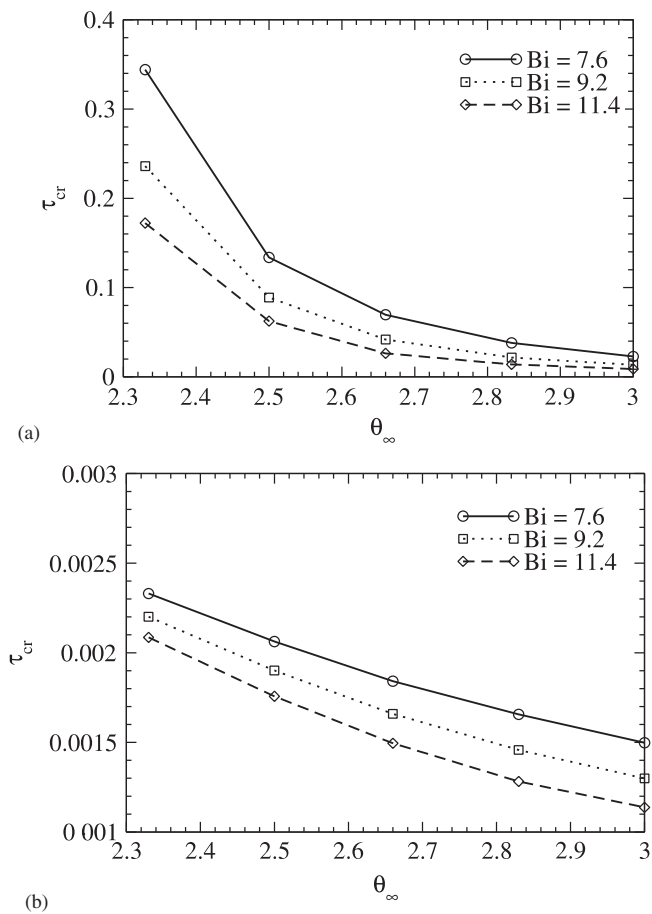


**Figure 5** Critical time against convective source temperature for different Biot numbers under (a) convective mode of heating and (b) combined convective and radiative mode of heating with  $\theta_h = 3$ .

similar to the situation wherein the wood is subjected to high velocity hot gases (Andrews, 2012; Cruz et al., 2006; Defraeye et al., 2011; Tan et al., 2009). From Figures 5a and 5b, it is evident that the larger the Bi number, the smaller the critical time for both convective and mixed mode heating. A comparison of Figures 5a and 5b reveals that the addition of radiation mode to the convection mode of heating, results in a reduction in critical time by an order of magnitude in the considered cases.

Shown in Figure 6 is the critical time versus the radiative heating source temperature ( $\theta_h$ ). The range of temperature used here is chosen based on reported temperatures in wildland fires (Butler et al., 2004b). It is seen that when  $\theta_h$  is decreased from 3.66 to 3, the critical time increases six-fold from around 0.0005 to 0.003. The effect of adding convection to radiative heating changed as the radiant heat source's intensity increased. This decrease is around 20% at  $\theta_h = 3$ , while it is not as significant at larger values of  $\theta_h = 3.66$ .

Inclusion of chemical degradation of wood subject to convective, radiative, and mixed mode heating allows us to examine the temporal evolution of the MLR, which is a global parameter that measures the rate of thermal degradation of the material in the entire domain. Here, MLR is obtained by the calculation of the total formation rate of pyrolysate from the solid phase (Lautenberger and Fernandez-Pello, 2009).

The time evolution of MLR for different convection source temperatures and various Bi numbers under convective and combined modes of heating is shown in Figure 7. MLR starts with a zero value at  $\tau = 0$  in all cases, increases to reach a maximum value, and then slowly decreases in almost all cases shown. The entire process occurs much faster for cases with combined convective and radiative heating. The MLR peak values are much larger for these cases, compared to the ones in which heating mode is only convection. The ratio of the peak MLR in the mixed mode to that in the convective mode ranges from about 4.6 for Bi = 7.6 to about 2.1 for Bi = 11.4. It is seen in Figure 7 that the influence of the change of the Bi number on how MLR evolves, is minimal for cases where convective heating is combined with radiative heating; however, as can be seen, this influence is significant under convective mode heating only. The overall effect of the increase of  $\theta_\infty$  is to increase the maximum of the MLR and to decrease the time of its occurrence in all cases. In cases where radiative heating is present, shortly after the MLR has peaked, the MLR curves for

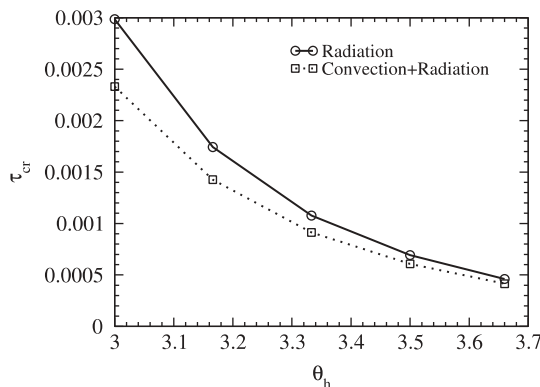


**Figure 6** Critical time against heater temperature in (a) radiative mode of heating and (b) combined radiative and convective mode of heating with  $\theta_\infty = 2.33$  and Bi = 7.6.

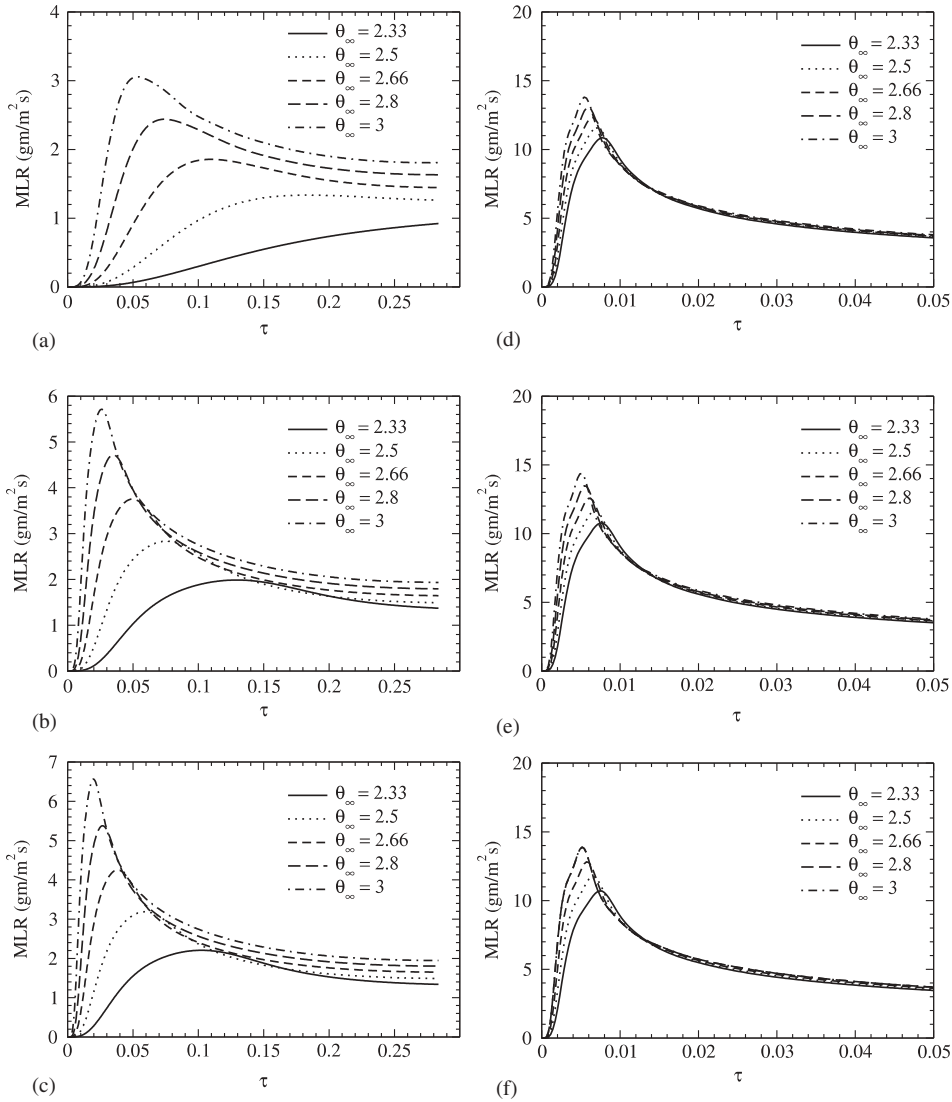


**Figure 7** Time evolution of mass loss rate in  $\text{g/m}^2/\text{s}$  for convective mode of heating (left column) and combined convective and radiative mode of heating with  $\theta_h = 3$  (right column); (a, d)  $\text{Bi} = 7.6$ ; (b, e)  $\text{Bi} = 9.2$ ; and (c, f)  $\text{Bi} = 11.4$ .

different values of  $\theta_\infty$  converge. This observation, that the MLR evolution is not sensitive to the variation of  $\text{Bi}$  in these cases, suggests that convection heating is suppressed by the radiative heating after an initial stage ( $\tau > 0.01$ ).

The time evolution of the MLR is shown for various radiative heating source temperatures  $\theta_h$  in [Figure 8](#). With an increase of  $\theta_h$  from 3 to 3.66, it is seen that the peak MLR increases from around  $10 \text{ g/m}^2/\text{s}$  to above  $25 \text{ g/m}^2/\text{s}$ . A power regression ( $y = Ax^B$ ) for this peak value against  $\theta_h$  reveals that the peak MLR is correlated with  $\theta_h^{4.94}$  in the radiative mode of heating ([Figure 8a](#)) and with  $\theta_h^{4.70}$  in a combined mode of heating ([Figure 8b](#)). It is noted that the radiative heat flux is correlated with  $\theta_h^4$  when the heating source temperature

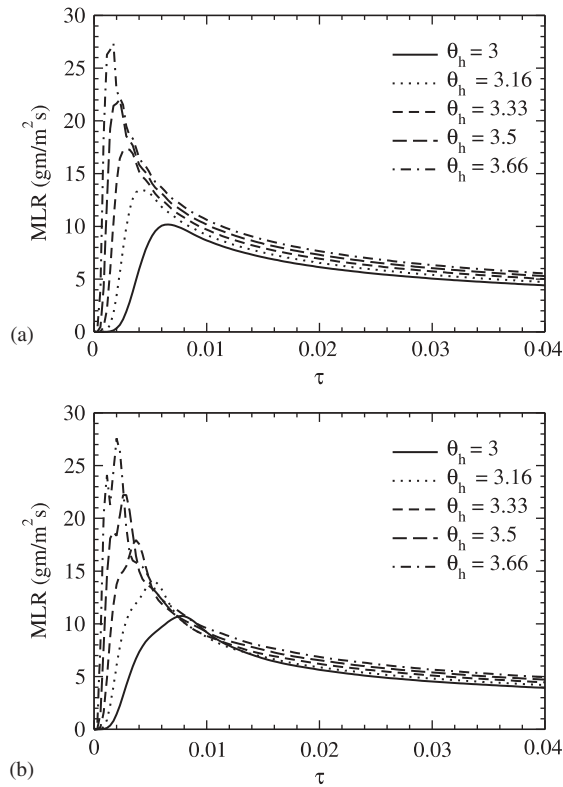


**Figure 8** Time evolution of the mass loss rate under (a) radiative mode of heating and (b) combined radiative and convective mode of heating with  $\theta_\infty = 2.33$  and  $Bi = 7.6$ .

is much larger than the surface temperature. A comparison between a typical curve of a constant  $\theta_\infty$  in Figure 8a and its counterpart in Figure 8b reveals that the addition of the convection mode to the radiation mode increases the MLR only slightly. This increase is obviously attributed to the fact that the overall energy transferred to the solid fuel is greater in Figure 8a compared to that in Figure 8b. Yet, the addition of the convection mode seems to have other effects including the widening of the peak of MLR and the shift in its time of occurrence to earlier times.

Figure 9 shows the charring rate versus position. Charring rate is a quantity that provides an insight into the char formation rate and its dependence on external heating. Char formation is a result of thermal degradation of the material (Bryden et al., 2002). Here, charring rate for a computational cell is computed by

$$\text{charring rate} = \frac{x_{0.9}^i - x_{0.9}^{i+1}}{t_{0.9}^i - t_{0.9}^{i+1}}$$

where  $i$  and  $i + 1$  denote adjacent cell numbers,  $x_{0.9}^i$  and  $x_{0.9}^{i+1}$  are the  $x$  coordinates of the cell centers in dimensional terms, and  $t_{0.9}^i$  and  $t_{0.9}^{i+1}$  denote the moments at which the char mass fractions of cells  $i$  and  $i + 1$  exceed 0.9. In all cases, the charring rate starts from around 0.01 mm/s at the dimensionless coordinate  $\xi = 0$ , then decreases slightly and reaches a

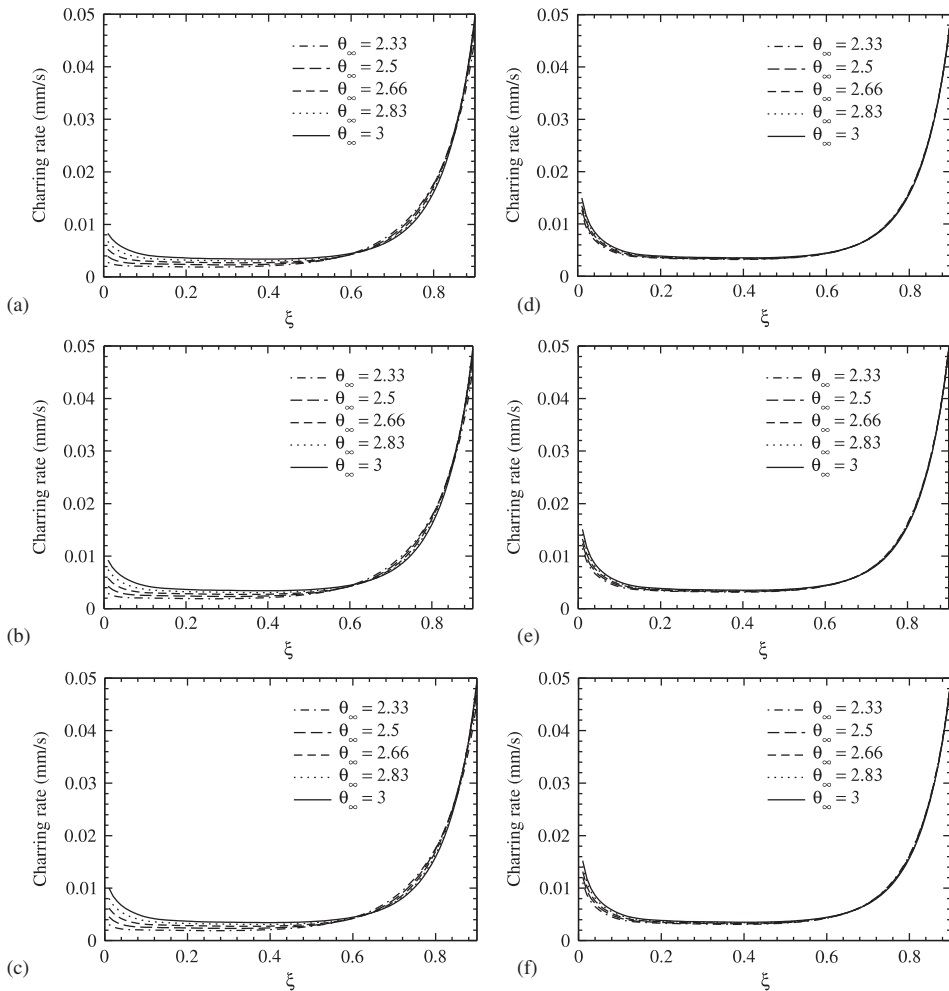


**Figure 9** Charring rate in mm/s plotted as a function of dimensionless position,  $\xi$  in convective mode of heating (left column) and combined convective and radiative mode of heating with  $\theta_\infty = 3$  (right column) for (a, d)  $Bi = 7.6$ ; (b, e)  $Bi = 9.2$ ; and (c, f)  $Bi = 11.4$ .

plateau that extends from around  $\xi = 0.1$  to around  $\xi = 0.6$ . Then it starts increasing until it reaches about 0.05 mm/s at  $\xi = 1.0$ . Starting values of the charring rate are somewhat smaller for smaller values of  $\theta_\infty$  in pure convection cases. As seen in the right panels, the variation of  $\theta_\infty$  in cases where there is radiative heating in addition to convection has little influence on the behavior of the charring rate. The variation of  $Bi$  number does not seem to have much influence on the behavior of the charring rate either. The charring rate starts out high because the region close to the left boundary is closer to the heating source and its temperature rises fast. On the other hand, the heating rate in the midsection of the slab is smaller and, due to this, charring rates are smaller in this region. As the char layer thickens, the heat transfer rate into the unreacted wood slows down (Bryden et al., 2002) and this explains the lower charring rate observed in the midsection. The increase in charring rate

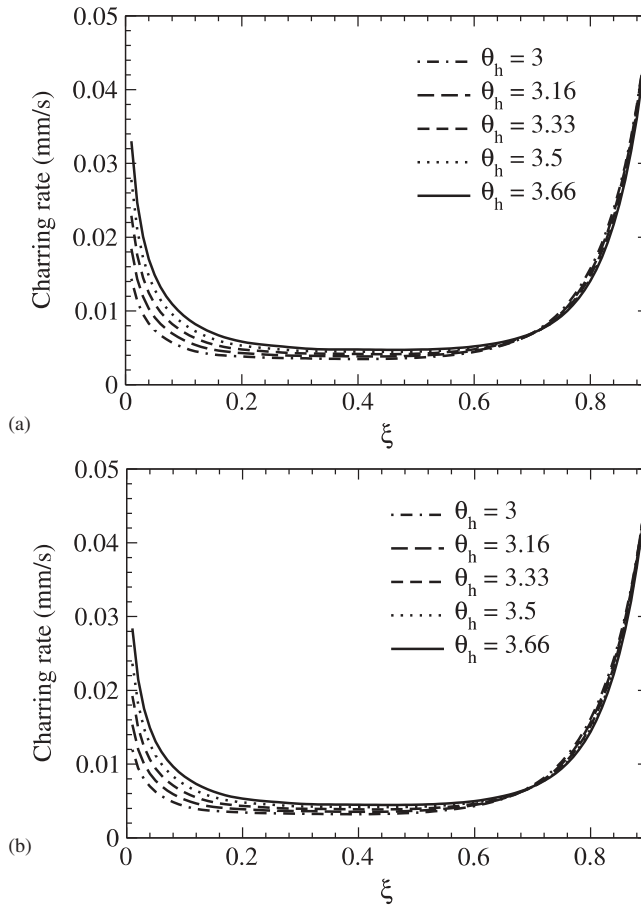


**Figure 10** Charring rate in mm/s vs. dimensionless position  $\xi$  under (a) radiative mode of heating and (b) combined radiative and convective mode of heating with  $\theta_\infty = 2.33$  and  $Bi = 7.6$ .

towards the end of the domain could be a result of low heat transfer in the regions closer to the right boundary, which is an insulated boundary condition.

The charring rate is plotted against  $\xi$  in Figure 10 for different values of  $\theta_h$ . The trends of the curves in this figure are similar to the ones shown in Figure 9. However, the initial behavior of the charring rate seen in Figure 10 is highly dependent on  $\theta_h$ . The charring rate between  $0 < \xi < 0.2$  is substantially smaller for smaller values of  $\theta_h$ . On the other hand, for  $\xi > 0.6$  the difference between the charring rates at different values of  $\theta_h$  is insignificant. Comparing the charring rate values in Figure 10a to the ones in Figure 10b reveals that the addition of the convective mode to the radiation mode of heating results in a small reduction in the charring rate.

## 5. SUMMARY AND CONCLUSIONS

Numerical investigation of the influence of convective, radiative, and mixed mode heating on critical time, mass loss rate, and charring rate was carried out for a slab of

wood using a general pyrolysis model, Gpyro. A one-step model approximation for wood degradation was validated initially with experimental results of Ohlemiller et al. (1987) and numerical results of Lautenberger and Fernandez-Pello (2009). During the investigation, temperatures of convective and radiative heating sources were assumed different when both modes of heating were present. Furthermore, the Bi number was changed from one case to another to understand the impact of the variations of these parameters on the wood pyrolysis process.

The increase in convective source temperature of 7% and Bi number of 17% reduces the critical time by 15% and 8%, respectively, during combined convective and radiative heating, illustrating that the increase in convective source temperature in the presence of radiation, does affect the surface heating of a material prior to ignition. However, the effect of Bi number on critical time was small. The increase in radiation source temperature by 5% during mixed mode heating in the presence of a constant convective source results in the decrease of critical times by 35%. These cases clearly indicate the balance between the two modes of heating during the preheating period of wood in a wildland fire scenario. In order to study the effects of heating once ignition takes place, MLR and charring rate were extensively investigated. As the MLR is a global quantity, it shows marginal variation during the mixed mode heating when the convective temperature and Biot numbers were increased by 7% and 17%, respectively. In the case of charring rate, during mixed mode heating, the charring rate is independent of heating rate used and is identical at all convective source temperatures and is also insensitive to changes in Bi number. However, it was found that the time advancements of MLR and charring rate experience negligible changes when a convection mode is added to the radiation mode. These observations suggest that the MLR and charring rate behave differently. In summary, the effect of heating modes and the balance between them during the preheating of a material and after its ignition have been carefully investigated. The heating rate and heating mode significantly affect the preheating of a material with convection playing a definite role while radiation predominantly heats the material owing to its faster heating rate. However, once the material ignites, then any variation in convective heating in the presence of radiation has a minimal effect on MLR and charring rates. The results summarized above could benefit wildland fire research by addressing the thermal behavior of unburned vegetation subjected to unsteady heating during an advance of a spreading fire. Although the setup studied here was geometrically simple, the modeled thermochemical processes, including the thermal degradation of fuel, and convection and diffusion of the generated gases within the fuel, were quite comprehensive, close to what happens to the solid fuel in wildland fires.

## ACKNOWLEDGMENT

The authors wish to thank Christopher W. Lautenberger for providing assistance on configuring and using Gpyro.

## ORCID

D. R. Weise  <http://orcid.org/0000-0002-9671-7203>

## FUNDING

The authors gratefully acknowledge the financial support from the Joint Fire Science Program and the USDA Forest Service PSW Research Station through cooperative agreement 11-JV-11272167-103 with The University of Alabama in Huntsville.

## REFERENCES

- Anderson, H.E. 1969. Heat transfer and fire spread. Res. Pap. INT-RP-69. U.S. Department of Agriculture, Forest Service, Intermountain Forest and Range Experiment Station, Ogden, Utah.
- Anderson, W.R., Catchpole, E.A., and Butler, B.W. 2010. Convective heat transfer in fire spread through fine fuel beds. *Int. J. Wildland Fire*, **19**, 284–298.
- Andrews, P.L. 2012. Modeling wind adjustment factor and midflame wind speed for Rothermel's surface fire spread model. General Technical Report RMRS-GTR-266, U.S. Department of Agriculture, Forest Service, Rocky Mountain Research Station, Fort Collins, CO.
- Atreya, A., Carpentier, C., and Harkleroad, M. 1986. Effect of sample orientation on piloted ignition and flame spread. In *Fire Safety Science, Proceedings of the 1st International Symposium*, International Association for Fire Safety Science, London.
- Babrauskas, V. 2001. Ignition of wood: A review of the start of the art. *J. Fire Prot. Eng.*, **12**, 163–189.
- Babu, B.V., and Chaurasia, A.S. 2003. Modeling for pyrolysis of solid particle: Kinetics and heat transfer effects. *Energy Convers. Manage.*, **44**, 2251–2275.
- Benkoussas, B., Consalvi, J.L., Porterie, B., Sardoy, N., and Loraud, J.C. 2007. Modeling thermal degradation of woody fuel particles. *Int. J. Therm. Sci.*, **46**, 319–327.
- Bergman, T.L., Lavine, A.S., Incropera, F.P., and Dewitt, D.P. 2011. *Fundamentals of Heat and Mass Transfer*, 7th ed., Wiley, Hoboken, NJ.
- Bilbao, R., Mastral, J.F., Lana, J.A., Ceamanos, J., Aldea, M.E., and Betran, M.A. 2002. Model for the prediction of the thermal degradation and ignition of wood under constant and variable heat flux. *J. Anal. Appl. Pyrolysis*, **62**, 63–82.
- Brescianini, C.P., Delichatsios, M.A., and Webb, A.K. 2003. Mathematical modeling of time to ignition in the early fire hazard test. *Combust. Sci. Technol.*, **175**, 319–331.
- Bryden, K.M., Ragland, K.W., and Rutland, C.J. 2002. Modeling thermally thick pyrolysis of wood. *Biomass Bioenergy*, **22**, 41–53.
- Butler, B.W., Cohen, J., Latham, D.J., Schuette, R.D., Sopko, P., Shannon, K.S., Jimenez, D., and Bradshaw, L.S. 2004a. Measurements of radiant emissive power and temperatures in crown fires. *Can. J. For. Res.*, **34**, 1577–1587.
- Butler, B.W., Finney, M.A., Andrews, P.L., and Albin, F.A. 2004b. A radiation-driven model for crown fire spread. *Can. J. For. Res.*, **34**, 1588–1599.
- Cruz, M.G., Butler, B.W., Alexander, M.E., and Viegas, D.X. 2006. Development and evaluation of a semi-physical crown fire initiation model. *For. Ecol. Manage.*, **234S**, S96.
- Defraeye, T., Blocken, B., and Carmeliet, J. 2011. Convective heat transfer coefficients for exterior building surfaces: Existing correlations and CFD modeling. *Energy Convers. Manage.*, **52**(1), 512–522.
- Delichatsios, M. A. 2005. Piloted ignition times, critical heat fluxes and mass loss rates at reduced oxygen atmospheres. *Fire Saf. J.*, **40**, 197–212.
- Delichatsios, M., Paroz, B., and Bhargava, A. 2003. Flammability properties for charring materials, *Fire Saf. J.*, **38**, 219–228.
- Dupuy, J. L. 2000. Testing two radiative physical models for fire spread through porous forest fuel beds. *Combust. Sci. Technol.*, **155**, 149–180.
- Ferguson, S.C., Dahale, A.R., Shotorban, B., Mahalingam, S., and Weise, D.R. 2013. The role of moisture on combustion of pyrolysis gases in wildland fires. *Combust. Sci. Technol.*, **185**, 435–453.

- Finney, M.A., Cohen, J.D., McAllister, S.S., and Jolly, W.M. 2013. On the need for a theory of wildland fire spread. *Int. J. Wildland Fire*, **22**, 25–36.
- Frankman, D., Webb, B.W., Butler, B.W., and Latham, D.J. 2010. Fine fuel heating by radiant flux. *Combust. Sci. Technol.*, **182**, 215–230.
- Gpyro 0.775. 2007. SVN 92. Available at: <http://reaxengineering.com/trac/gpyro>.
- Haseli, Y., van Oijen, J.A., and H de Goeij, L.P. 2012. Analytical solutions for prediction of the ignition time of wood particles based on a time and space integral method. *Thermochim. Acta*, **548**, 65–75.
- Lautenberger, C.W., and Fernandez-Pello, A.C. 2005. Approximate analytical solutions for the transient mass loss rate and piloted ignition time of a radiatively heated solid in the high heat flux limit. *Fire Saf. Sci.*, **8**, 445–456.
- Lautenberger, C.W., and Fernandez-Pello, A.C. 2009. A model for the oxidative pyrolysis of wood. *Combust. Flame*, **156**, 1503–1513.
- Lawson, D.I., and Simms, D.L. 1952. The ignition of wood by radiation. *Br. J. Appl. Phys.*, **10**, 288–292.
- Lizhong, Y., Zaifu, G., Yupeng, Z., and Weicheng, F. 2007. The influence of different external heating ways on pyrolysis and spontaneous ignition of some woods. *J. Anal. Appl. Pyrolysis*, **78**, 40–45.
- McAllister, S., Finney, M., and Cohen, J. 2011. Critical mass flux for flaming ignition of wood as a function of external radiant heat flux and moisture content. Presented at the 7th US National Technical Meeting of the Combustion Institute, Georgia Institute of Technology, Atlanta, Georgia, March 20–23.
- McAllister, S., Grenfell, I., Hadlow, A., Jolly, W.M., Finney, M., and Cohen, J. 2012. Piloted ignition of live forest fuels. *Fire Saf. J.*, **51**, 133–142.
- Moghtaderi, B., Novozhilov, V., Fletcher, D., and Kent, J.H. 1997. A new correlation for bench scale piloted ignition data of wood. *Fire Saf. J.*, **29**, 41–59.
- Ohlemiller, T.J., Kashiwagi, T., and Werner, K. 1987. Wood gasification at fire level heat fluxes. *Combust. Flame*, **69**, 155–170.
- Pagni, P.J., and Peterson, T.G. 1973. Flame spread through porous fuels. *Symp. (Int.) Combust.*, **14**, 1099–1107.
- Rasbash, D.J., Drysdale, D.D., and Deepak, D. 1986. Critical heat and mass transfer at pilot ignition and extinction of a material. *Fire Saf. J.*, **10**, 1–10.
- Rothermel, R.C., and Anderson, H.E. 1966. Fire spread characteristics determined in the laboratory. Res. Pap. INT-RP-30. U.S. Department of Agriculture, Forest Service, Intermountain Forest and Range Experiment Station, Ogden, Ut.
- Shen, D.K., Fang, M.X., and Chow, W.K. 2006. Ignition of wood-based materials by thermal radiation. *Int. J. Eng. Perform.-Based Fire Codes*, **8**, 69–83.
- Simms, D.I., and Law, M. 1960. The ignition of wet and dry wood by radiation. *Combust. Flame*, **11**, 293–300.
- Tan, Z., Su, G., and Sub, J. 2009. Improved lumped models for combined convective and radiative cooling of a wall. *Appl. Therm. Eng.*, **29**, 2439–2443.
- Thomson, H.E., Drysdale, D.D., and Beyler, C.L. 1988. An experimental evaluation of critical surface temperature as a criterion for piloted ignition of solid fuels. *Fire Saf. J.*, **13**, 185–196.
- Weber, R.O. 1991. Modeling fire spread through fuel beds. *Prog. Energy Combust. Sci.*, **17**, 67–82.
- Zhou, X., Mahalingam, S., and Weise, D.R. 2005. Modeling of marginal burning state of fire spread in live chaparral shrub fuel bed. *Combust. Flame*, **143**(3), 183–198.